PHREEQC evaporation simulations

PHREEQC (Parkhurst and Appelo, 1999) evaporation simulations using the Pitzer equation were carried out to evaluate the minerals formed from evaporating seawater with varying Mg and SO_4 concentrations as would have occurred during the Phanerozoic (Hardie, 1996). The composition of the input solutions in the evaporation models solutions (2-20mM Mg, 5-15mM SO_4, 10.5mM Ca 10.4mM K, 558mM Cl and Na was adjusted to charge balance the solutions, Table DR1) were within the chemical range of the experimental solutions (Table 1). In addition, the Phanerozoic seawater composition from both calcite and aragonite seas, including compositions between these end members (8mM SO_4, 30mM Ca and 29mM Mg to 29mM SO_4, 10mM Ca and 54mM Mg, Horita et al., 2002; Table DR2) were also used as input solutions in the evaporation simulations. The simulations were run by removing increasing amounts of H_2O from the solutions and allowing precipitation (Table DR3). All simulated solutions contained Ca, Mg, SO_4, Na, Cl, CO_3 and K to allow precipitation of all major evaporite minerals, listed in Table DR4, during the simulations (Hardie, 1996).

A summary of results from the PHREEQC modeling are presented in Table DR1 and DR2. Fig. DR1-DR4 and DR9 show the evolution of the solution composition as a function of the remaining water as modeled by PHREEQC and Fig. DR5-DR8 and Fig. DR10 show the occurrence of the evaporite minerals in equilibrium with the evaporated solutions (Fig. DR1-DR4 and DR9). The evaporite type (Hardie, 1996) was determined by examining the evaporite mineral sequence (Table DR1, DR2, DR4 and Figure DR5-DR8 and DR10). When sylvite, and/or $CaCl_2$ minerals (Table DR4) were present during the evaporation of the modeled solutions in the absence of $MgSO_4$ minerals the evaporite type was determined to be KCl, and the evaporite type was determined to be $MgSO_4$ when polyhalite, and/or kieserite were present during the evaporation of the modeled solutions (Hardie, 1996). For the purpose of this publication we included the $MgSO_4$ + KCl evaporite type in the $MgSO_4$ type because both of these evaporite types were coincident with the aragonite seas (Hardie, 1996). The sea type (e.g. Lowenstein et al., 2003) was determined from the composition of the final invariant solution (Table DR1 and DR2); when the Ca concentration exceeded the SO_4 concentration the sea type was determined to be $CaCl_2$ and when the SO_4 concentration exceeded the Ca concentration the sea type was determined to be $MgSO_4$. Using the chemical divide that e.g. Lowenstein et al. (2003) used does not result in the same sea type that the final invariant solution suggest. According to Lowenstein et al. (2003) the $CaSO_4$ chemical divide, when the calcium and sulphate concentrations are equal in seawater, is the chemical boundary condition between different evaporite types i.e. when the calcium concentrations is less than the sulfate concentration sulfate is left in the evaporating solution and magnesium sulfate evaporites (e.g. kieserite, Table DR4) are able to precipitate resulting in a $MgSO_4$ evaporite sequence originating from a $MgSO_4$ sea. However, this does not take into account the precipitation of $CaCl_2$ minerals like antarcticite and tachyhydrite (Table DR1 and DR2 and Fig. DR1 to DR10), which form in addition to $CaSO_4$ minerals. This removes additional Ca from solution, therefore the Ca/SO_4 ratio at which additional SO_4 remains in solution to form $MgSO_4$ evaporites is >1.(e.g. in a seawater solution with initial [Ca] =10.5mM, the calculated chemical divide, separating between $MgSO_2$ and KCl evaporite types occurred at ~9mM SO_4, Table DR1).

Table DR1. Table with input and output solutions from the evaporation simulations on solutions in the concentration range from the experimental set-up, including the sea type (Lowenstein et al., 2003), the evaporite type (Hardie, 1996) and the evaporite mineral sequence as they occur in the simulations

Simulation run	Starting composition of modeled solutions (mM)							Composition of the final invariant solutions (mol/kg)							Sea type*	Evaporite type#	Evaporite mineral sequence§
	Ca	Mg	SO_4	Na	Cl	K	DIC	Ca	Mg	SO_4	Na	Cl	K	DIC			
1	10.5	2	5	535	558	10.4	2.47	6.84	0.551	1.19E-05	0.031	15.1	0.312	9.81E-05	$CaCl_2$	KCl	Cc, G, A, H, Syl, Car, Ant
2	10.5	2	8	541	558	10.4	2.47	6.84	0.551	1.19E-05	0.031	15.1	0.312	9.81E-05	$CaCl_2$	KCl	Cc, G, A, H, Syl, Car, Ant
3	10.5	2	10	545	558	10.4	2.47	0.00268	4.52	0.154	0.46	8.93	0.492	0.367	$MgSO_4$	$MgSO_4$	Cc, G, A, H, Syl, Pol, Car
4	10.5	2	15	555	558	10.4	2.47	0.00817	0.305	0.33	4.9	6.87	2.011	0.00715	$MgSO_4$	$MgSO_4$	Cc, G, A, H, Gl, Pol, Syl
5	10.5	5	5	529	558	10.4	2.46	6.84	0.551	1.19E-05	0.031	15.1	0.312	9.81E-05	$CaCl_2$	KCl	Cc, G, A, H, Syl, Car, Ant
6	10.5	5	8	535	558	10.4	2.46	6.84	0.551	1.19E-05	0.031	15.1	0.312	9.81E-05	$CaCl_2$	KCl	Cc, G, A, H, Syl, Car, Ant
7	10.5	5	10	539	558	10.4	2.46	0.00268	4.52	0.154	0.46	8.93	0.492	0.367	$MgSO_4$	$MgSO_4$	Cc, G, A, H, Syl, Pol, Car
8	10.5	5	15	549	558	10.4	2.46	0.00268	4.52	0.154	0.46	8.93	0.492	0.367	$MgSO_4$	$MgSO_4$	Cc, G, A, H, Gl, Pol, Syl, Car
9	10.5	10	5	519	558	10.4	2.45	6.84	0.551	1.19E-05	0.031	15.1	0.312	9.81E-05	$CaCl_2$	KCl	Cc, G, A, H, Syl, Car, Ant
10	10.5	10	8	525	558	10.4	2.45	6.84	0.551	1.19E-05	0.031	15.1	0.312	9.81E-05	$CaCl_2$	KCl	Cc, G, A, H, Syl, Car, Ant
11	10.5	10	10	529	558	10.4	2.45	0.00268	4.52	0.154	0.46	8.93	0.492	0.367	$MgSO_4$	$MgSO_4$	Cc, G, A, H, Syl, Pol, Car
12	10.5	10	15	539	558	10.4	2.45	0.000784	6.81	0.319	0.253	9.4	0.174	1.978	$MgSO_4$	$MgSO_4$	Cc, G, A, H, Gl, Pol, Syl, Car, Ki
13	10.5	20	5	499	558	10.4	2.43	5.22	2.54	3.94E-06	0.019	15.6	0.0221	0.000233	$CaCl_2$	KCl	Cc, G, A, H, Syl, Car, Bi, Tac
14	10.5	20	8	505	558	10.4	2.43	5.22	2.54	3.94E-06	0.019	15.6	0.0221	0.000233	$CaCl_2$	KCl	Cc, G, A, H, Syl, Car, Bi, Tac
15	10.5	20	10	509	558	10.4	2.43	0.00113	8.72	0.0467	0.0744	11.7	0.0184	2.802	$MgSO_4$	$MgSO_4$	Cc, G, A, H, Syl, Car, Bi, Ki
16	10.5	20	15	519	558	10.4	2.43	0.00113	8.72	0.0467	0.0744	11.7	0.0184	2.802	$MgSO_4$	$MgSO_4$	Cc, G, A, H, Pol, Syl, Car, Ki, Bi

* The sea type was determined from the invariant solutions where Ca>SO4 represents a CaCl2 type sea and Ca<SO4 represents a MgSO4 type sea.

The evaporite type is determined from the evaporite mineral sequence; when sylvite is present without any MgSO4 mineral the evaporite type is KCl and when polyhalite and/or kieserite is present the evaporite type is MgSO4 (Hardie, 1996)

§ The evaporite mineral sequences are determined from Fig. DR5-8; the abbreviations of the mineral phases and their chemical formula are listed in Table DR4.

Table DR2. Table with input and output solutions from the evaporation simulations on solutions between the cretaceous and the present day chemistry as proposed by for example Horita et al. (2003), including the sea type (Lowenstein et al., 2003), the evaporite type (Hardie, 1996) and the evaporite mineral sequence as they occur in the simulations

Simulation run	Starting composition of modeled solutions (mM)							Composition of the final invariant solutions (mol/kg)							Sea type*	Evaporite type#	Evaporite mineral sequence§
	Ca	Mg	SO4	Na	Cl	K	DIC	Ca	Mg	SO4	Na	Cl	K	DIC			
17	10.5	54.3	28.9	478	558	10.4	2.37	0.00113	8.72	0.0467	0.0744	11.7	0.0184	2.8	MgSO4	MgSO4	Cc, G, A, H, Gl, Pol, E, Hx, Ki, Car, Bi
18	13.8	50	25.3	473	558	10.4	2.37	0.00113	8.72	0.0467	0.0744	11.7	0.0184	2.8	MgSO4	MgSO4	Cc, G, A, H, Pol, Car, Ki, Bi
19	19.2	43	19.6	465	558	10.4	2.36	0.00113	8.72	0.0467	0.0744	11.7	0.0184	2.8	MgSO4	MgSO4	Cc, G, A, H, Syl, Car, Bi, Ki
20	20.8	41	17.9	462	558	10.4	2.36	5.22	2.54	3.94E-06	0.019	15.6	0.0221	0.000233	CaCl2	KCl	Cc, G, A, H, Syl, Car, Bi, Tac
21	25.4	35	13	455	558	10.4	2.35	5.22	2.54	3.94E-06	0.019	15.6	0.0221	0.000233	CaCl2	KCl	Cc, G, A, H, Syl, Car, Bi, Tac
22	29.9	29	8	448	558	10.4	2.18	5.9	2.06	3.72E-06	0.0164	16	0.0306	0.000178	CaCl2	KCl	Cc, G, A, H, Syl, Car, Bi, Tac, Ant

* The sea type was determined from the invariant solutions where Ca>SO4 represents a CaCl2 type sea and Ca<SO4 represents a MgSO4 type sea.

The evaporite type is determined from the evaporite mineral sequence; when sylvite is present without any MgSO4 mineral the evaporite type is KCl and when polyhalite and/or kieserite is present the evaporite type is MgSO4 (Hardie, 1996)

§ The evaporite mineral sequences are determined from Fig. DR10; the abbreviations of the mineral phases and their chemical formula are listed in Table DR4.

Table DR3. The first 77 lines of one input file for the PHREEQC evaporation calculations; additional lines were added to continuously removing water from the solutions saved in the previous part from the model.

```
phases
Tachyhydrite
CaMg2Cl6:12H2O = Ca+2 + 2Mg+2 + 6Cl- + 12H2O
log_k 17.1439
Antarcticite
CaCl2:6H2O = Ca+2 + 2Cl- + 6H2O
log_k 4.0933

selected_output
-water true
-distance false
-time false
-file Z:\Min-Gro\experiments\constant addition\PHREEQC-evaporation\m2-15.xls
-totals S(6) Ca Mg K Na Cl C(4)
-equilibrium_phases halite sylvite antarcticite bischofite tachyhydrite carnallite gypsum anhydrite epsomite hexahydrite kieserite polyhalite glauberite calcite
-saturation_indices halite sylvite antarcticite bischofite tachyhydrite carnallite gypsum anhydrite epsomite hexahydrite kieserite polyhalite glauberite calcite

solution 1
-pH 7
-Temp 21
-water 1
reaction 1
MgCl2       2.0
Na2SO4      15.0
NaCl        522.6
CaCl2       10.5
KCl         10.4
NaHCO3  2
Na2CO3  0.3
0.001
equilibrium_phases 1
halite 0 0
sylvite 0 0
antarcticite 0 0
bischofite 0 0
tachyhydrite 0 0
carnallite 0 0
gypsum 0 0
anhydrite 0 0
epsomite 0 0
hexahydrite 0 0
kieserite 0 0
polyhalite 0 0
glauberite 0 0
calcite 1 0
CO2(g) -3.412 10000
save solution 1
save equilibrium_phases 1
end

solution 2
save solution 2
end

mix 1
1           1
2           -0.1
use equilibrium_phases 1
save solution 1
save equilibrium_phases 1
end

mix 2
1           1
2           -0.09
use equilibrium_phases 1
save solution 1
save equilibrium_phases 1
end

mix 3
1           1
2           -0.0405
use equilibrium_phases 1
save solution 1
save equilibrium_phases 1
end
```

Table DR4. List with possible evaporite minerals, their abbreviation as used in Table DR1 and DR2 and their chemical formula.

Mineral	Abbreviation	Chemical formula
calcite	Cc	$CaCO_3$
gypsum	G	$CaSO_4 \cdot 2H_2O$
anhydrite	A	$CaSO_4$
halite	H	NaCl
sylvite	Syl	KCl
carnallite	Car	$KMgCl_3 \cdot 6H_2O$
antarcticite	Ant	$CaCl_2 \cdot 6H_2O$
tachyhydrite	Tac	$CaMg_2Cl_6 \cdot 12H_2O$
bischofite	Bi	$MgCl_2 \cdot 6H_2O$
glauberite	Gl	$Na_2Ca(SO_4)_2$
polyhalite	Pol	$K_2Ca_2Mg(SO_4)_4 \cdot 2H_2O$
epsomite	E	$MgSO_4 \cdot 7H_2O$
hexahydrite	Hx	$MgSO_4 \cdot 6H_2O$
kieserite	Ki	$MgSO_4 \cdot H_2O$

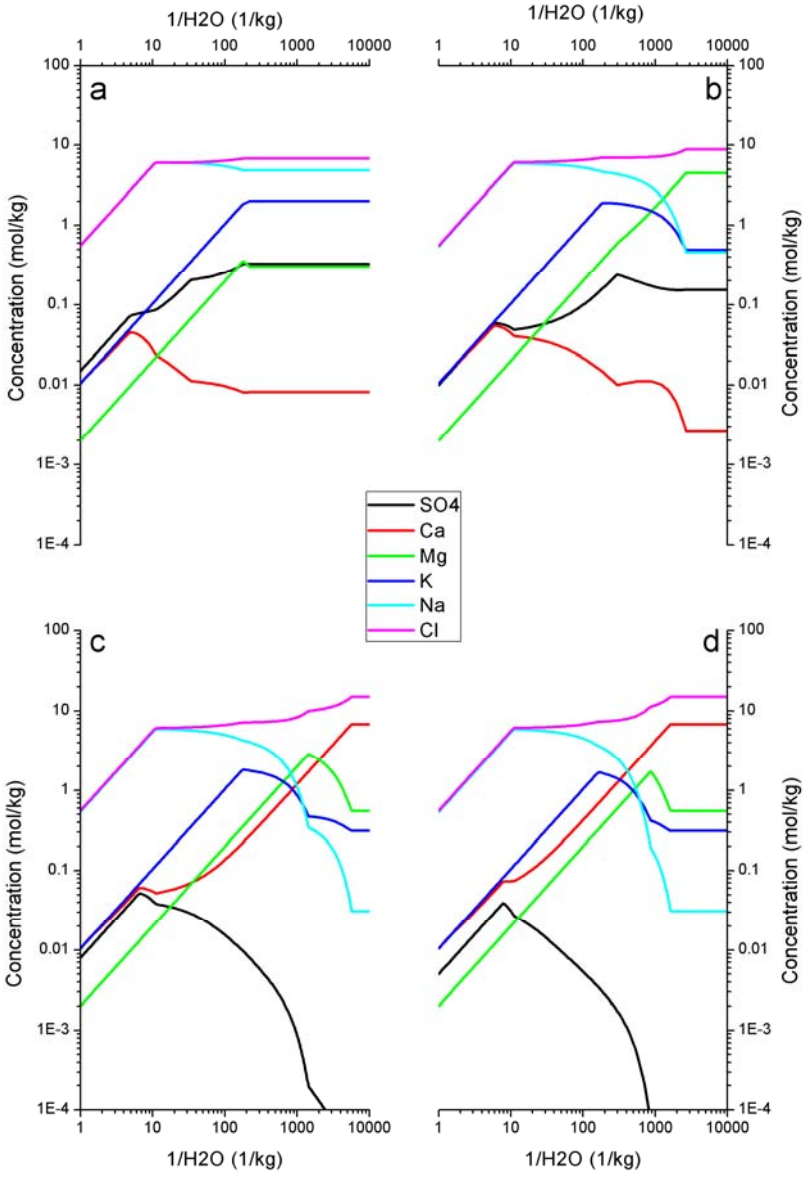

Figure DR1. The evolution of the solution from simulation runs 1-4; 2mM Mg and a. 15mM SO_4, b. 10mM SO_4, c. 8mM SO_4 and d. 5mM SO_4 (table DR1).

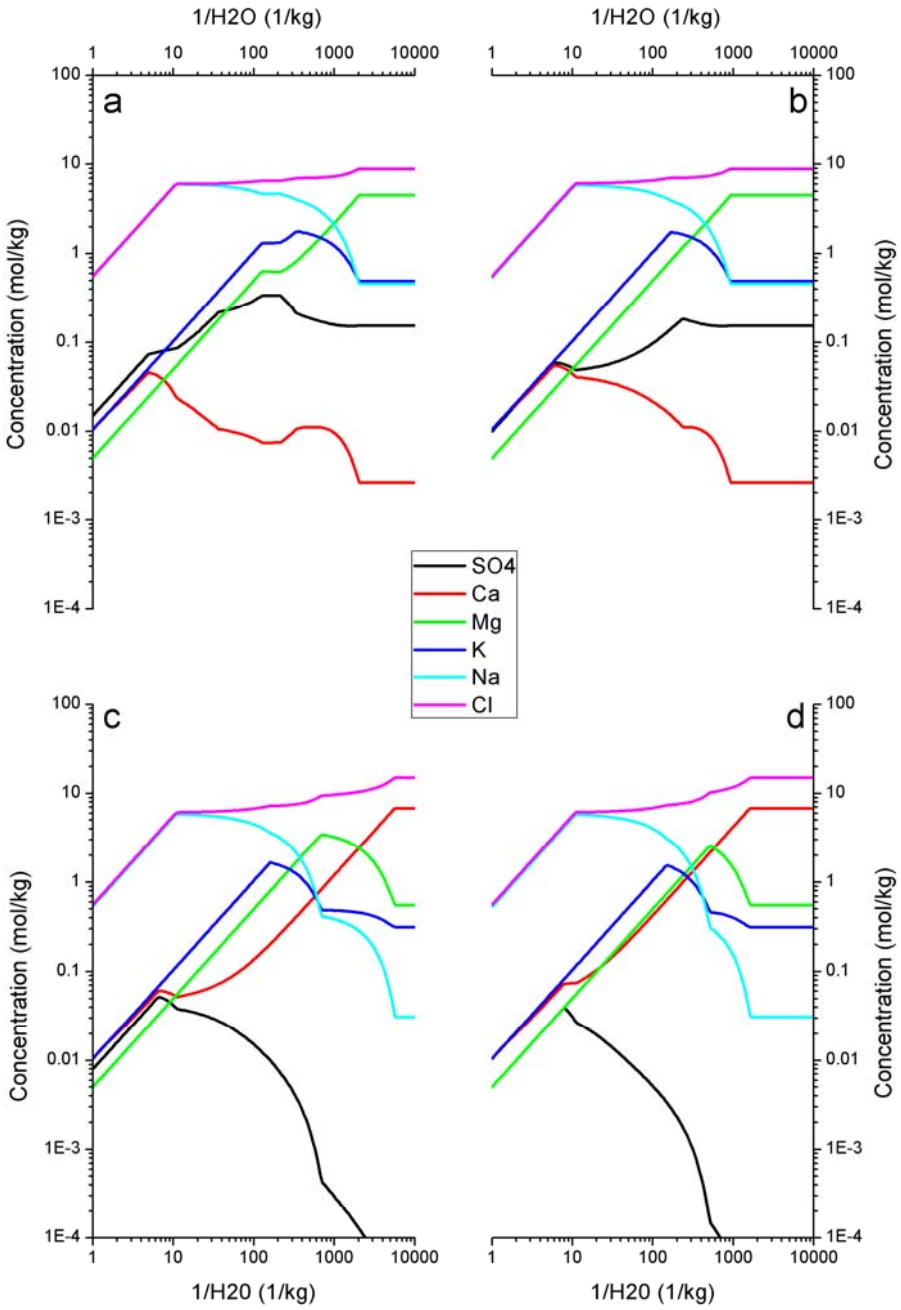

Figure DR2. The evolution of the solution from simulation runs 2-8; 5mM Mg and a. 15mM SO_4, b. 10mM SO_4, c. 8mM SO_4 and d. 5mM SO_4 (table DR1).

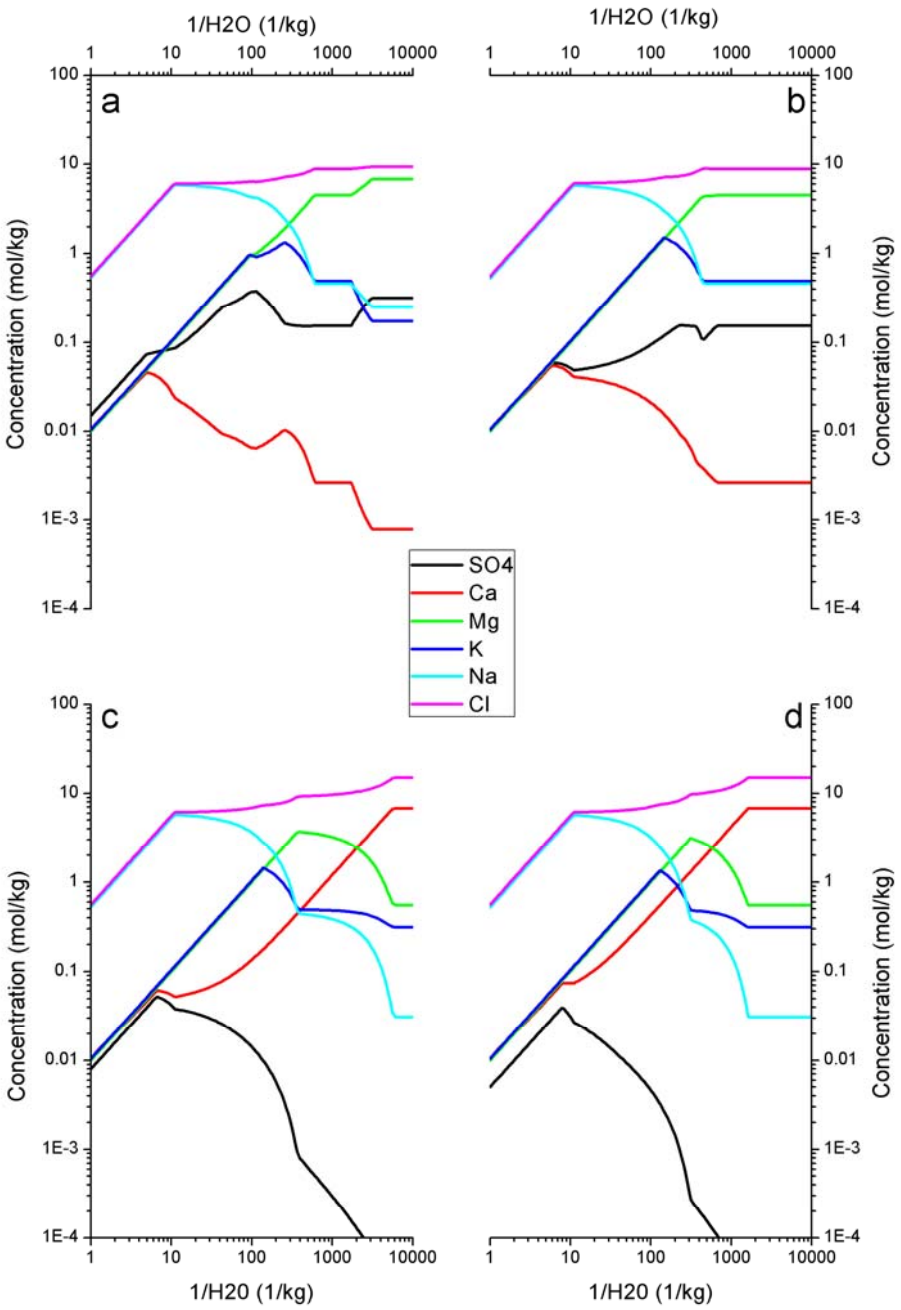

Figure DR3. The evolution of the solution from simulation runs 9-12; 10mM Mg and a. 15mM SO_4, b. 10mM SO_4, c. 8mM SO_4 and d. 5mM SO_4 (table DR1).

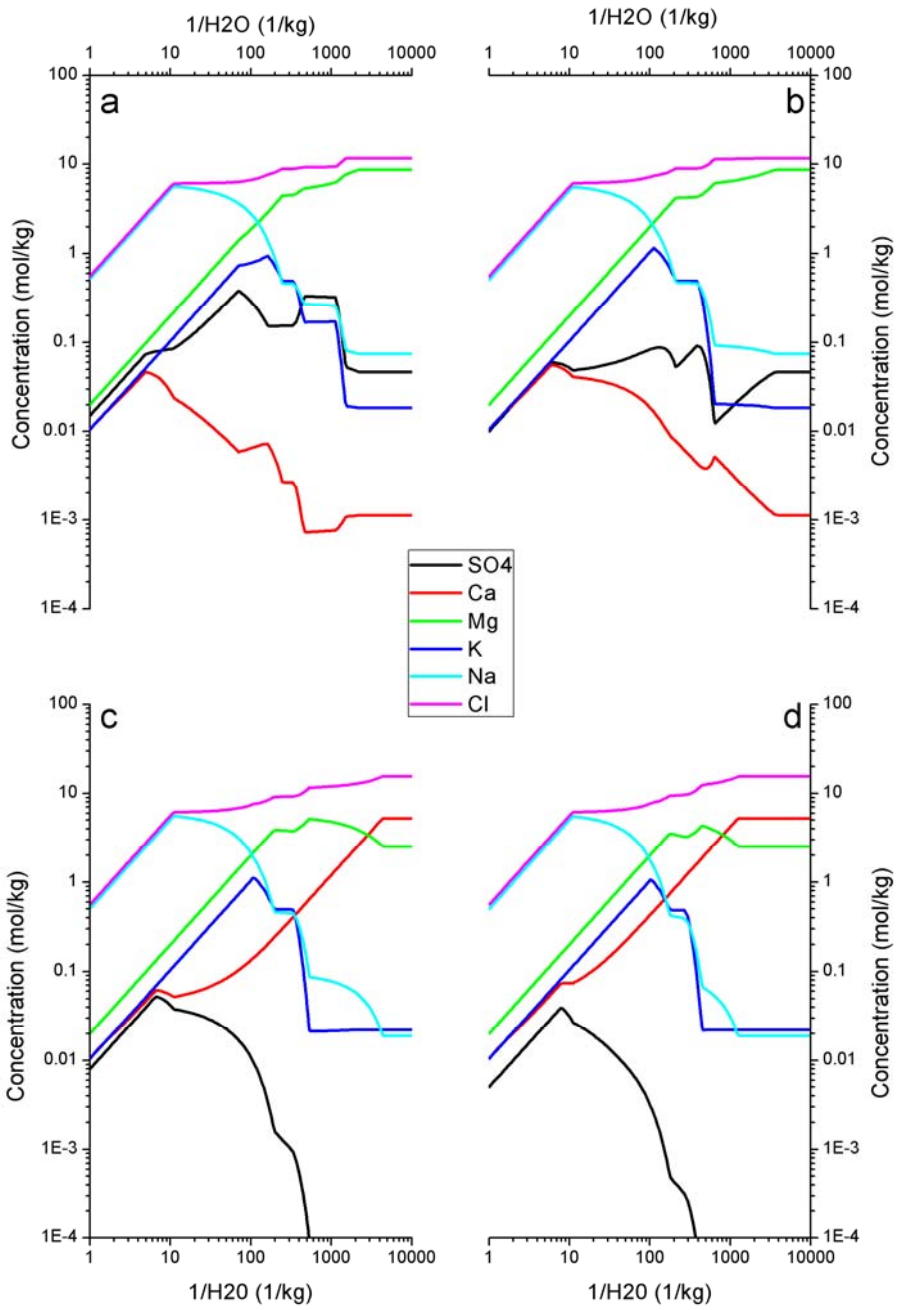

Figure DR4. The evolution of the solution from simulation runs 13-16; 20mM Mg and a. 15mM SO_4, b. 10mM SO_4, c. 8mM SO_4 and d. 5mM SO_4 (table DR1).

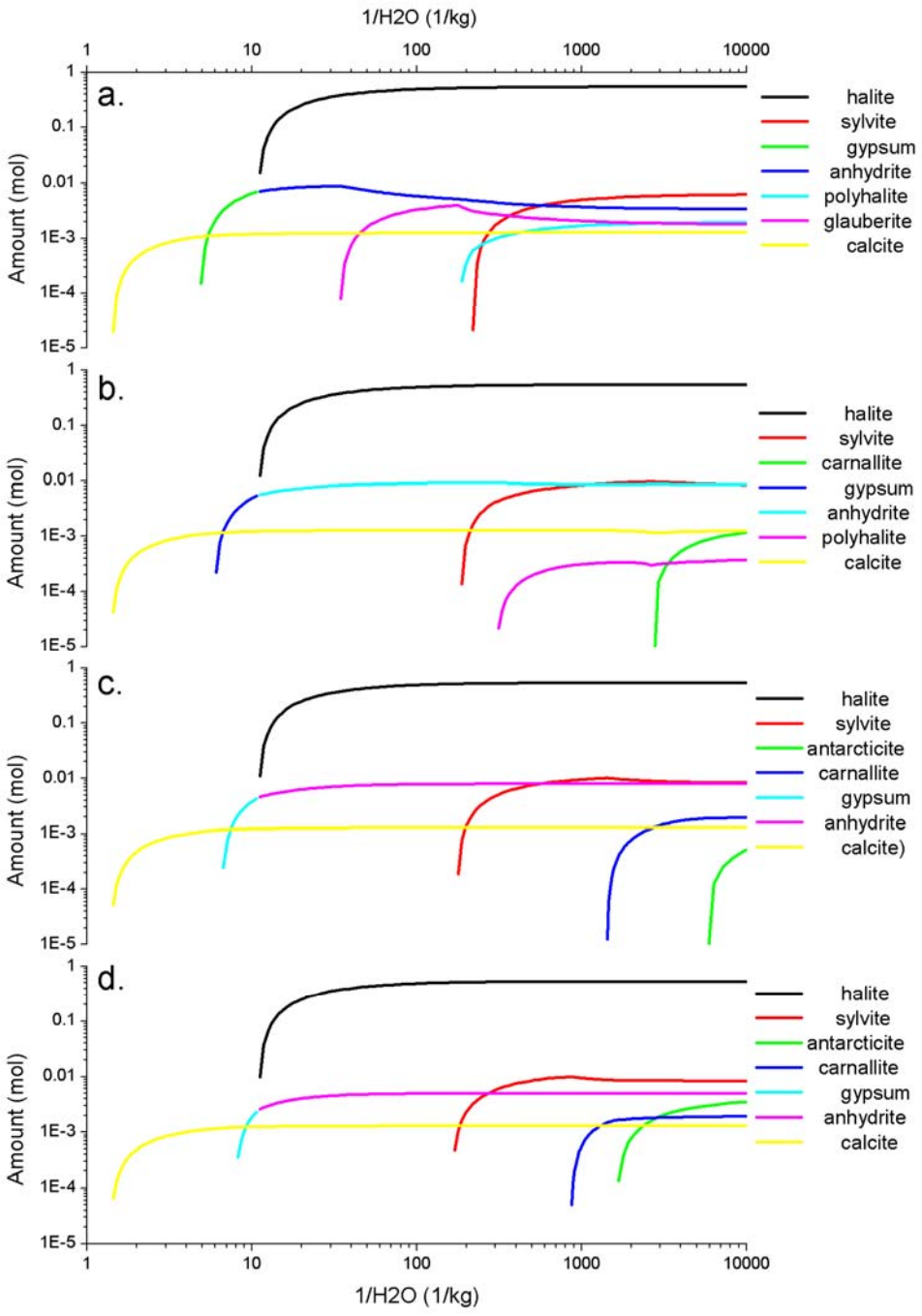

Figure DR5. The evaporite sequence from simulation runs 1-4; 2mM Mg and a. 15mM SO_4, b. 10mM SO_4, c. 8mM SO_4 and d. 5mM SO_4 (table DR1); note that the color coding for the mineral phases is not the same in each graph it is dependent on the evaporite sequence.

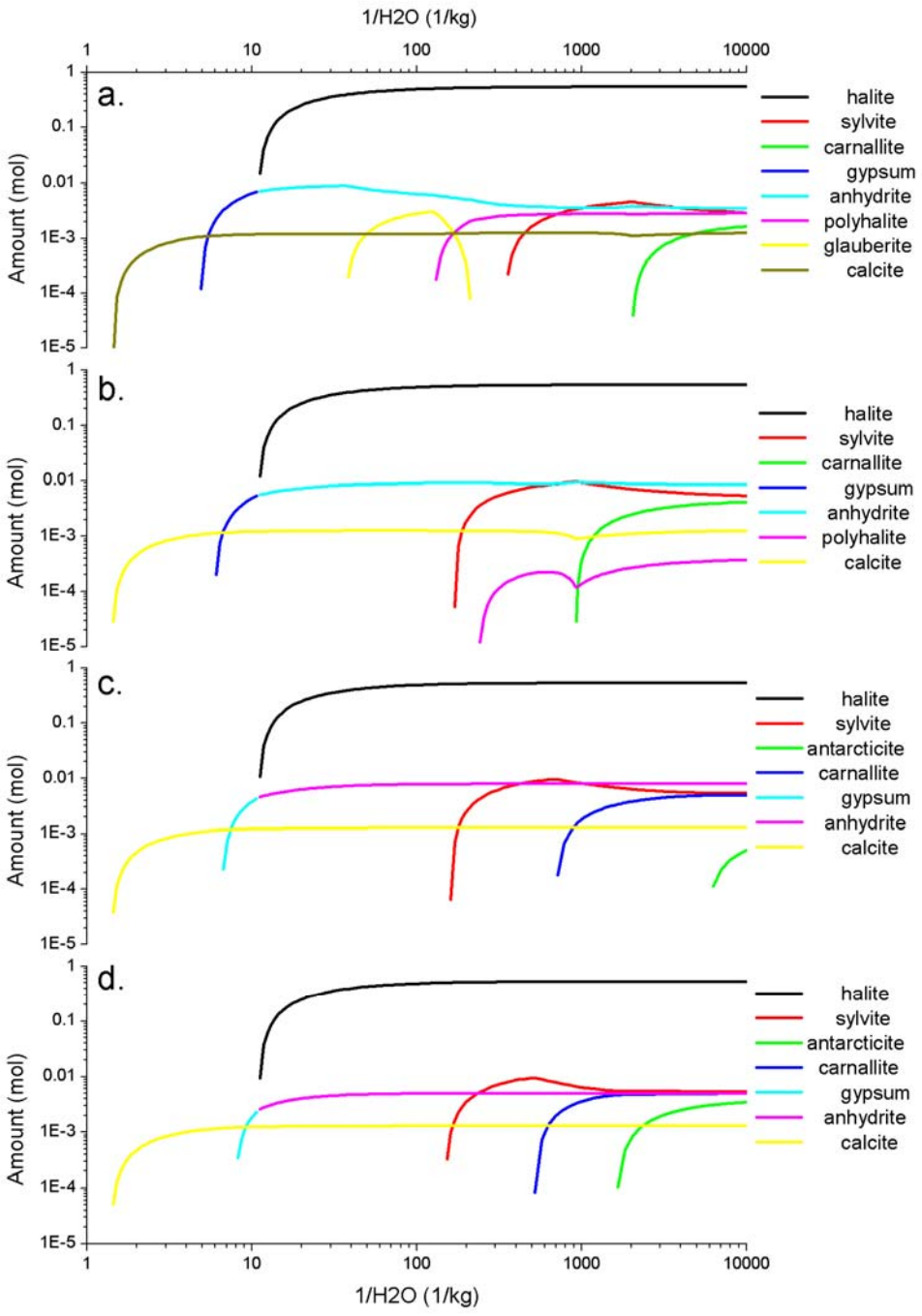

Figure DR6. The evaporite sequence from simulation runs 5-8; 5mM Mg and a. 15mM SO_4, b. 10mM SO_4, c. 8mM SO_4 and d. 5mM SO_4 (table DR1); note that the color coding for the mineral phases is not the same in each graph it is dependent on the evaporite sequence.

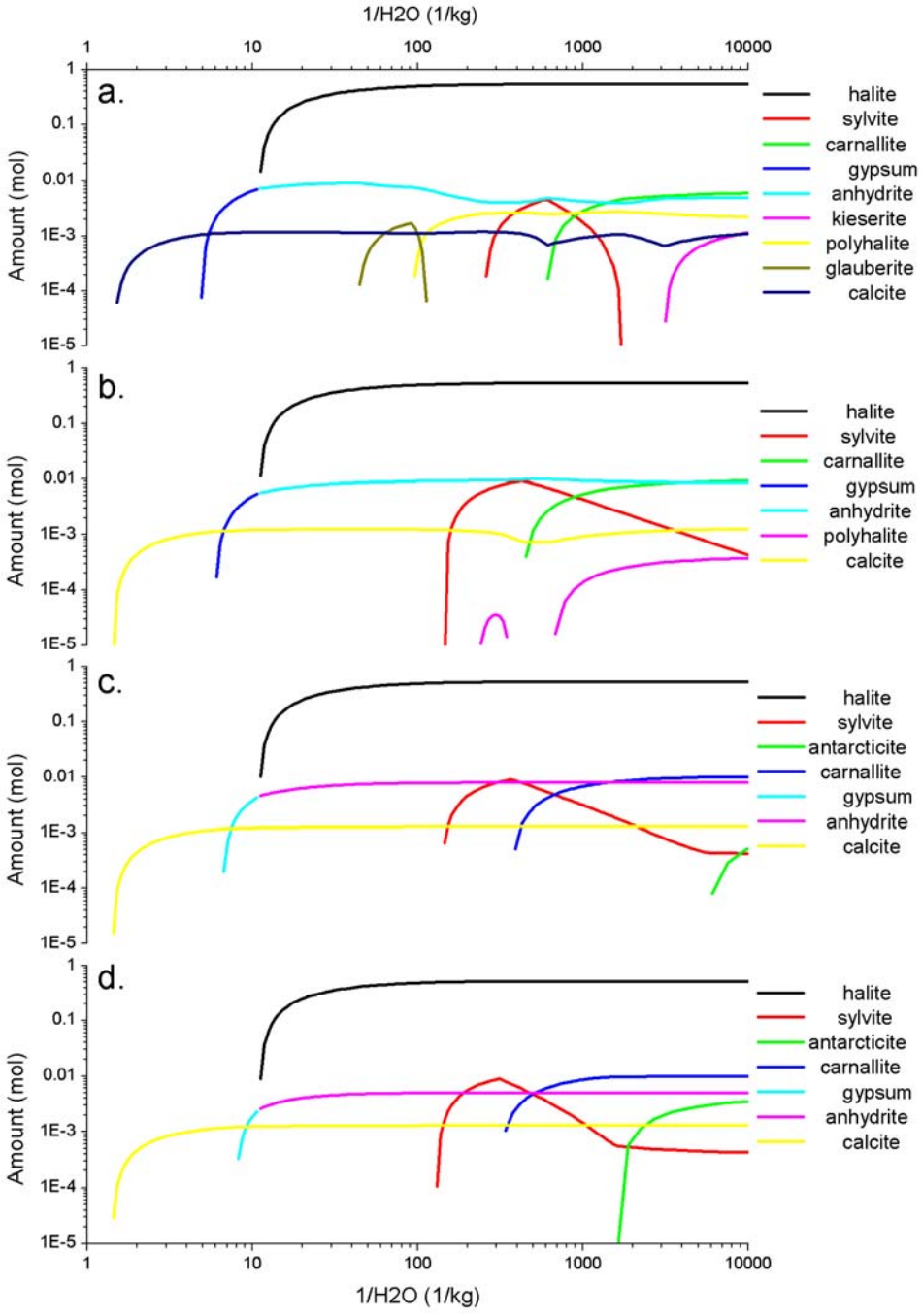

Figure DR7. The evaporite sequence from simulation runs 9-12; 10mM Mg and a. 15mM SO_4, b. 10mM SO_4, c. 8mM SO_4 and d. 5mM SO_4 (table DR1); note that the color coding for the mineral phases is not the same in each graph it is dependent on the evaporite sequence.

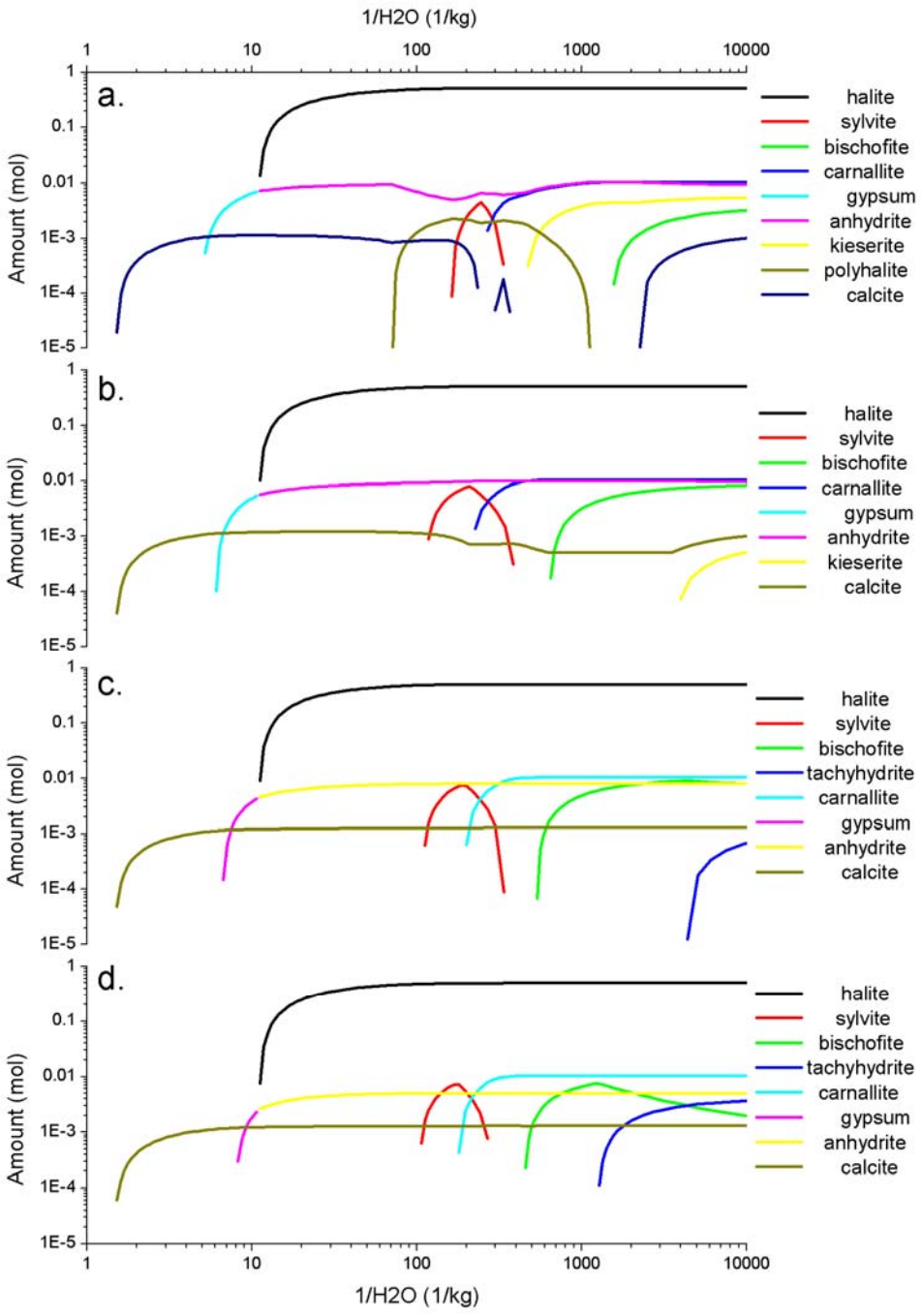

Figure DR8. The evaporite sequence from simulation runs 13-16; 20mM Mg and a. 15mM SO_4, b. 10mM SO_4, c. 8mM SO_4 and d. 5mM SO_4 (table DR1); note that the color coding for the mineral phases is not the same in each graph it is dependent on the evaporite sequence.

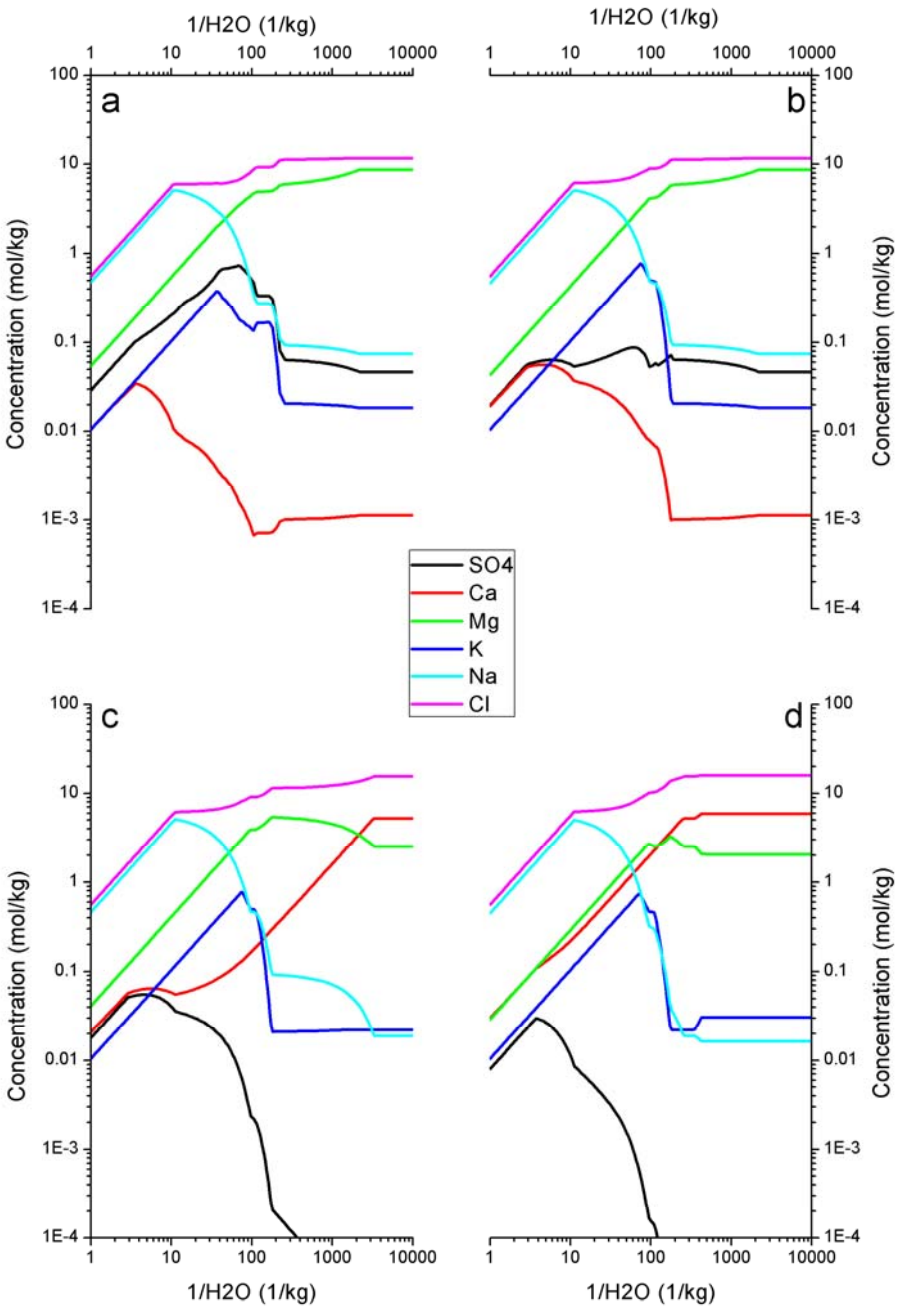

Figure DR9. The evolution of the solution from simulation runs a: 17, b: 19, c: 20 and d: 22 (Table DR2).

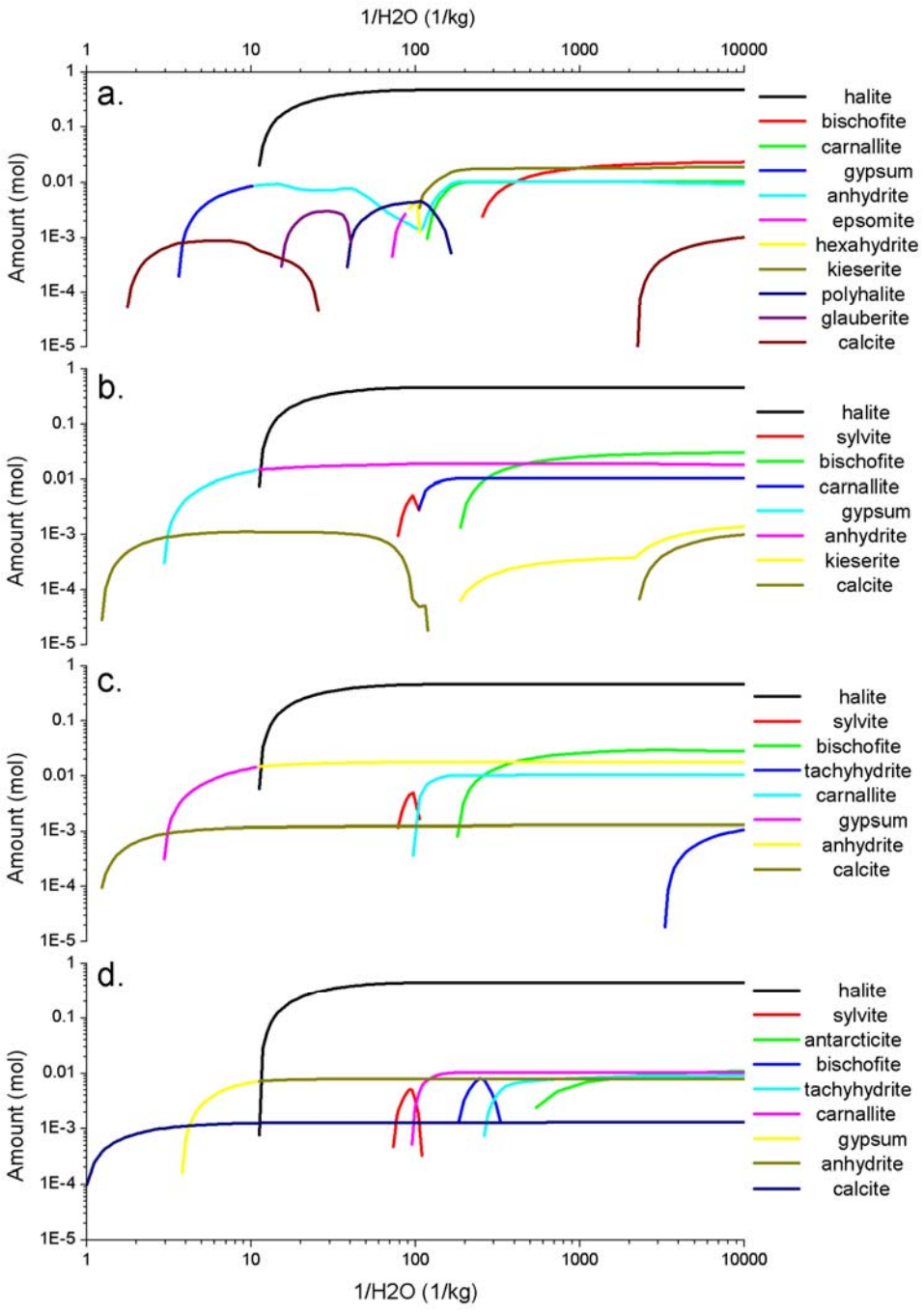

Figure DR10. The evaporite sequence from simulation runs a: 17, b: 19, c: 20 and d: 22 (Table DR2); note that the color coding for the mineral phases is not the same in each graph it is dependent on the evaporite sequence.

Validation of the experimental method

Throughout the constant addition experiments, the solution chemistry (Mg, SO4 and Ca, Table 1) remained constant (±5%). This is in contrast to free drift experiments (e.g., Morse et al., 1997) in which major changes in solution chemistry occur during $CaCO_3$ formation (e.g, significant increases in Mg/Ca, Morse et al., 1997). The $CaCO_3$ was precipitated onto glass spheres to mimic abiotic ooid formation in the ocean. In addition, the solids were imaged using a Field Emission Gun Scanning Electron Microprobe (FEG-SEM) to obtain morphological information (Fig. DR11). $CaCO_3$ precipitated on the glass spheres show similar features compared to natural aragonite and calcite oöids, where aragonite crystals precipitated tangentially on the glass spheres (Fig. 11DRa-c) and calcite crystals radially (Fig. 11DRd-e) (e.g., Simone, 1980; Wilkinson et al., 1984). This emphasizes the applicability of our experimental approach to closely mimic abiotic $CaCO_3$ mineral formation in Phanerozoic seawater.

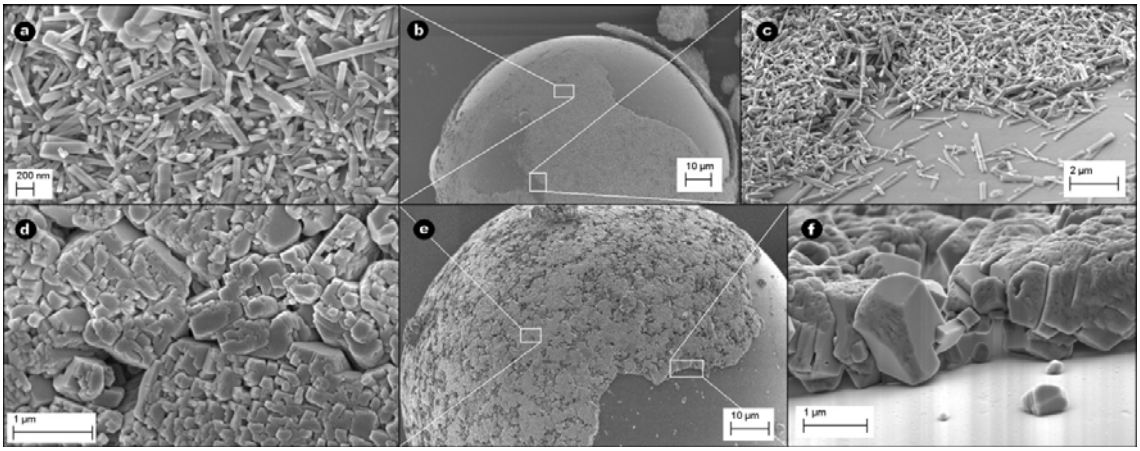

Figure DR11. FEG-SEM images of aragonite (a-c) and calcite (d-e) precipitated on glass spheres.

Mucci and Morse (1983) determined that saturation state and precipitation kinetics do not influence the incorporation of Mg into calcite. This indicates that the mineral phases formed during the experiments were not influenced by the different absolute Ca (10mM) concentration used compared to proposed Phanerozoic seawater concentrations (up to 30mM Ca, Horita et al., 2002). During the first 2–3h of each experiment the injection of the $NaCO_3$ solutions caused the pH to increase to ~8.9. This was a consequent of an increase in alkalinity from ~1.8mM to ~4.5mM due to the lack of $CaCO_3$ precipitation. The initiation of $CaCO_3$ precipitation caused the pH to decrease rapidly and stabilize at ~8.2. Such a temporary increase in alkalinity has no significant effect on $CaCO_3$ precipitation (Lee and Morse, 2010). Finally, model predictions for seawater alkalinity during the Phanerozoic (~2-~7mM, Mackenzie et al., 2008) do not differ significantly from the alkalinity during our experiments (~1.8mM), and Lee and Morse (2010) showed no significant effect on the precipitation on $CaCO_3$ within this range of alkalinities (1-7mM).

References

Hardie, L.A., 1996, Secular variation in seawater chemistry: An explanation for the coupled secular variation in the mineralogies of marine limestones and potash evaporites over the past 600 my: Geology, v. 24, p. 279-283.

Horita, J., Zimmermann, H., and Holland, H.D., 2002, Chemical evolution of seawater during the Phanerozoic: Implications from the record of marine evaporites: Geochimica et Cosmochimica Acta, v. 66, p. 3733-3756.

Lee, J., and Morse, J.W., 2010, Influences of alkalinity and pCO_2 on $CaCO_3$ nucleation from estimated Cretaceous composition seawater representative of "calcite seas": Geology, v. 38, p. 115-118.

Lowenstein, T.K., Hardie, L.A., Timofeeff, M.N., and Demicco, R.V., 2003, Secular variation in seawater chemistry and the origin of calcium chloride basinal brines: Geology, v. 31, p. 857-860.

Mackenzie, F.T., Arvidson, R.S., and Guidry, M., 2008, Phaerozoic time chemostatic modes of the ocean-atmosphere-sediment system through Phanerozoic time: Mineralogical Magazine, v. 72, p. 333-335.

Morse, J.W., Wang, Q.W., and Tsio, M.Y., 1997, Influences of temperature and Mg:Ca ratio on $CaCO_3$ precipitates from seawater: Geology, v. 25, p. 85-87.

Mucci, A., and Morse, J.W., 1983, The incorporation of Mg^{2+} and Sr^{2+} into calcite overgrowths: influences of growth rate and solution composition: Geochimica et Cosmochimica Acta, v. 47, p. 217-233.

Parkhurst, D.L., and Appelo, C.A.J., 1999, User's guide to PHREEQC (version 2) — a computer program for speciation, batch-reaction, one-dimensional transport, and inverse geochemical calculations: Denver, Colorado, U.S. Geological Survey p. 312.

Simone, L., 1980, Ooids: A review: Earth-Science Reviews, v. 16, p. 319-355.

Walter, L.M., 1986, Relative Efficiency of Carbonate Dissolution and Precipitation During Diagenesis: A Progress Report on the Role of Solution Chemistry, *in* Gautier, D.L., ed., Roles of Organic Matter in Sediment Diagenesis, Volume 38, Society of Economic Paleontologists and Mineralogists Special Publication p. 1-11.

Wilkinson, B.H., Buczynski, C., and Owen, R.M., 1984, Chemical control of carbonate phases; implications from Upper Pennsylvanian calcite-aragonite ooids of southeastern Kansas: Journal of Sedimentary Research, v. 54, p. 932-947.